Available online at www.sciencedirect.com

ScienceDirect

Mendeleev Commun., 2019, **29**,713–715

Mendeleev Communications

Ordered honeycomb-like network of $MnO_2 \cdot nH_2O$ nanocrystals formed on the surface of a $Mn(OAc)_2$ solution drop upon interaction with O_3 gas

Valeri P. Tolstoy, Nadezhda I. Vladimirova and Larisa B. Gulina*

Institute of Chemistry, St. Petersburg State University, 199034 St. Petersburg, Russian Federation. E-mail: l.gulina@spbu.ru

DOI: 10.1016/j.mencom.2019.11.039

Planar ordered honeycomb-like structures of the MnO_2 layered birnessite-type crystalline form have for the first time been synthesized on the surface of $Mn(OAc)_2$ solution drops upon interaction with O_3 gas. The obtained network consists of 2D nanocrystals of the thickness up to 10 nm. The prepared material possesses a hierarchical structure and can be used in a fabrication of advanced sensor and electrode materials.

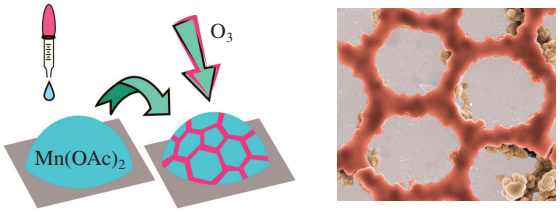

In recent years, a considerable interest has been drawn to obtaining and studying various ordered nanostructured materials formed at the interface between two phases due to interfacial reactions.[1–6] Investigations of such materials at the solid–liquid interface, including a liquid deposited as the drop on a solid surface, are recognized as one of the most important subjects in this field.[7,8] These works attract a considerable attention due to opportunities of their practical application. The processes of deposition and evaporation of solution droplets underlie 2D and 3D printing technologies and a method for producing electrodes in various electrochemical devices, *viz.*, drop-casting. Unique conditions and effects appear during the evaporation of droplets of various solutions and suspensions,[9,10] *e.g.*, the Marangoni and 'coffee ring' effects.[11] These effects lead to the structurization of resulting products.

In contrast to the most discussed processes of deposition and evaporation of a drop, the present work was aimed at the chemical interaction on the drop surface. Before drying, the drop surface was treated with a gaseous reagent according to the gas–solution interface technique (GSIT).† We have earlier employed this method to obtain nanocrystals, thin films and microtubes for many inorganic compounds.[12–15] Previous works[16,17] have revealed that a hydrophobic film of manganese(III, IV) oxide can be formed on a vessel surface upon the interaction of $Mn(OAc)_2$ solution with gaseous O_3 *via* GSIT in the vessel equipped with flat air interface. That material possesses a great potential for its practical application as electrode materials for chemical current sources, electrochemical sensors, catalysts for the oxidation of organic compounds, *etc.*[18–21] In this work, the reaction between O_3 gas and small (8–40 μl) droplets of $Mn(OAc)_2$ solution located on a glass surface resulted in a light brown film formed on the surface of solution drop. Once the drop has been dried, the obtained film was investigated using SEM, XRD, optical microscopy and other methods.‡

The first experiments demonstrated that a light brown film was formed on the surface of drop of a $Mn(OAc)_2$ solution upon its treatment with O_3 gas flow. Immediately after the reaction, this film was observed on the drop surface using an optical microscope in the transmission or reflection modes. The observations showed that the film contained separate intricate curved 'ribbons' with a width of 1–2 μm, while some of them formed a network of honeycomb structures consisting of the cells sized up to 20 μm in diameter (Figure 1). These cells possess both hexagonal and pentagonal shapes. Moreover, these shapes inside a single film structure are alternately arranged and form a continuous conjugated net similar to that of carbon atom cells in the fullerene structure or a sequence of fragments on the surface of soccer ball. Our results also demonstrate that these ordered structures are mainly located in the central

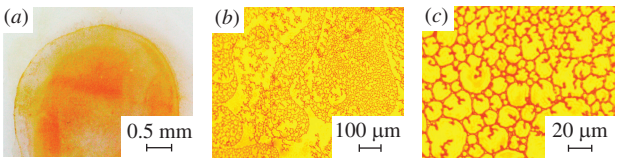

Figure 1 Optical images of a $Mn(OAc)_2$ solution drop after its treatment with O_3 for 10 min, acquired in transmission mode with different magnification.

† The starting $Mn(OAc)_2 \cdot 4H_2O$ (of chemically pure grade, Vekton) was used as received. Aqueous solutions were prepared using a high-purity H_2O (of resistivity > 18 MΩ cm, obtained using a Milli-Q system). The synthesis was carried out at ambient temperature. Drops of $Mn(OAc)_2$ solution of the concentration of 0.0025 mol dm^{-3} and volume of 8–40 μl were applied onto a glass surface and placed in a flow reactor (the diameter of 20 mm). A mixture of air and O_3 was fed into the reactor. The droplet diameter under these conditions was about 2–4 mm, and the contact angle was 50°. The air flow rate was 30 dm^3 h^{-1}. Before applying a drop of the solution, the glass surface was cleaned by treating with acetone in an ultrasonic bath. Ozone was produced by an OZ-1 M barrier-type pulse generator with an O_3 output of 0.4 g h^{-1}. The time of sample treatment with O_3 varied from 1 to 10 min.

‡ Optical data were acquired using a Biolam optical microscope (LOMO, Russia) and an Altami digital camera. The images were recorded both in transmission and reflection modes for the drop surfaces immediately after their interaction with O_3 and for the drops dried in air. The wetting angle was measured using an LK-1 goniometer (Open Science, Russia) at the accuracy of ±1°. The SEM images were taken on either a Zeiss EVO-40EP or a Zeiss Auriga microscopes. The X-ray powder diffraction analysis was carried out on a Bruker D2 Phaser diffractometer equipped with a CuKα X-ray source.

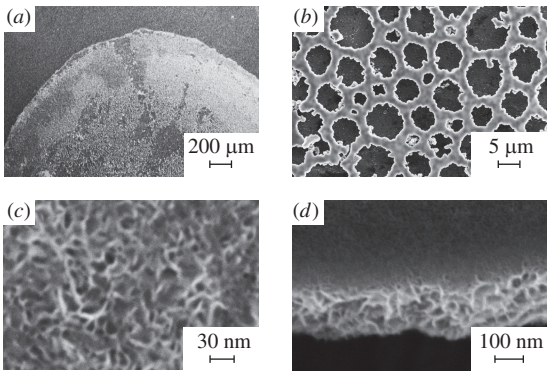

Figure 2 SEM images of the samples obtained *via* drying of previously O_3-treated (for 10 min) $Mn(OAc)_2$ solution drop: (*a*)–(*c*) top views at the different magnification and (*d*) the side view.

area of drops. It is important that the network of ordered structures is generally retained even after complete drying of the drop. Finally, the crystal growth and droplet evaporation processes take place at the same perimeter of the reaction zone with a decrease in the contact angle.

SEM images of dried droplets for the similar film (Figure 2) show that the film is a porous network formed from ribbons of width about 1–2 μm. The ribbons consist of individual planar nanocrystals of the thickness up to 10 nm, oriented mainly perpendicular to the solution–air interface [see Figure 2(*c*)]. As one can see from Figure 2(*d*), the thickness of such a ribbon is *ca.* 100 nm.

According to the X-ray powder diffraction data (Figure 3), the synthesized product was poorly crystallized. The broad peaks at 36.9 and 65.8° can be assigned to layered δ-MnO_2.[22,23]

Apparently, once a drop of $Mn(OAc)_2$ solution was contacted with O_3, a chemical process began on its surface. At the first step, a redox reaction occurs between O_3 molecules from the gaseous phase and Mn^{II} hydrated cations located on the liquid surface:

$$Mn(OAc)_2 + O_3 + (n+1)H_2O \rightarrow MnO_2{\cdot}nH_2O + 2AcOH + O_2 .$$

Hydrophobic nuclei of $MnO_2{\cdot}nH_2O$ nanocrystals are among the products of this reaction, which possess the uniform size and negative charge[24] and therefore, repulse each other forming a system of nanoparticles at the equal distances on the surface of solution. Consequently, O_3 molecules diffuse into the salt solution through the free interface, so the nanocrystals grow from the solution side, resulting in the occurrence of consolidation. The formation of such nanocrystals could be facilitated by convection flows, which were previously observed[10,25] in the droplet during its partial drying upon the contact with the air flow. These flows contribute to the mixing of the $Mn(OAc)_2$ solution and levelling its concentration in the drop volume.

In our view, the growth of array of $MnO_2{\cdot}nH_2O$ nanocrystals at the air–solution interface can be interpreted according to the

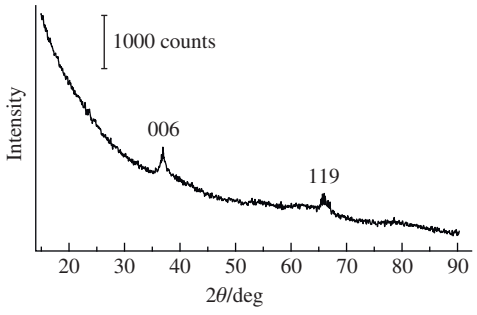

Figure 3 XRD for the powder of nanocrystals formed on the surface of O_3-treated $Mn(OAc)_2$ solution drop.

methodology for the formation of periodic colloidal structures[26] and the diffusion pattern model,[27,28] which describe the fractal growth of crystals under the conditions of simultaneously occurring chemical reaction and the process of diffusion of reagents into the reaction zone. Thus, conditions for an ordered periodic arrangement of the chemical reaction products may arise.

We hypothesize that the forces acting on the droplet surface due to its curvature can also play an important role in the formation of observed honeycomb structures. Among such forces, there are both gravity, which promotes the movement of nanocrystals 'down the slope' of the drop surface, and the force of convection currents occurring inside the drop and on its surface during the partial evaporation. The area of external surface of the drop decreases during the evaporation resulting in the increased forces of mutual repulsion of nanocrystals. All these surface interactions form unique 'force fields', which lead to the formation of ordered honeycomb structures. We assume that the mutual alternation of conjugate hexa- and pentagons in the continuous net of MnO_2 cells is an unique feature of the synthesized structure, which can only be realized on a convex surface according to geometry.

In conclusion, the synthetic conditions free of special surfactants and templates have been for the first time found for planar ordered honeycomb-like structures containing the cells sized few microns in the diameter and consisting of tightly packed oriented $MnO_2{\cdot}nH_2O$ nanoparticles of a hexagonal birnessite-type crystalline structure and a minimum size along the *c*-axis equal to 3–8 nm. It was suggested that the formation of these structures was caused by the redox reaction in a thin layer on the droplet surface, leading to the nanocrystals. The key feature in the ordering of these structures may be the action of additional 'force-fields' on the droplet surface.

There is no doubt that these cell-like structures possess a number of practically important properties and can be used, *e.g.*, to create new high-performance electrodes for electrochemical sensors.

This work was supported by the Russian Science Foundation (grant no. 16-13-10223-P). The XRD analysis and the SEM studies were carried out at the X-ray Diffraction and the Nanotechnology Centers of the Research Park at the St. Petersburg State University.

References

1 S.-Y. Zhang, M. D. Regulacio and M.-Y. Han, *Chem. Soc. Rev.*, 2014, **43**, 2301.
2 E. N. Golubina, N. F. Kizim, E. V. Sinyugina and I. N. Chernyshev, *Mendeleev Commun.*, 2018, **28**, 110.
3 V. P. Ananikov, *Mendeleev Commun.*, 2016, **26**, 1.
4 K. Ariga, M. V. Lee, T. Mori, X. Y. Yu and J. P. Hill, *Adv. Colloid Interface Sci.*, 2010, **154**, 20.
5 B. A. Noskov and A. G. Bykov, *Russ. Chem. Rev.*, 2015, **84**, 634.
6 E. O. Pentsak and V. P. Ananikov, *Mendeleev Commun.*, 2014, **24**, 327.
7 A. I. Rusanov, *Mendeleev Commun.*, 1996, **6**, 30.
8 O. I. Vinogradova and A. L. Dubov, *Mendeleev Commun.*, 2012, **22**, 229.
9 A. Accardo, M. Burghammer, E. D. Cola, M. Reynolds, E. D. Fabrizio and C. Riekel, *Langmuir*, 2011, **27**, 8216.
10 R. D. Deegan, O. Bakajin, T. F. Dupont, G. Huber, S. R. Nagel and T. A. Witten, *Nature*, 1997, **389**, 827.
11 L. E. Scriven and C. V. Sternling, *Nature*, 1960, **187**, 186.
12 L. Gulina, V. Tolstoy, L. Kuklo, V. Mikhailovskii, V. Panchuk and V. Semenov, *Eur. J. Inorg. Chem.*, 2018, 1842.
13 L. B. Gulina, V. P. Tolstoy, Y. V. Petrov and D. V. Danilov, *Inorg. Chem.*, 2018, **57**, 9779.
14 L. B. Gulina, V. P. Tolstoy, I. A. Kasatkin and Y. V. Petrov, *J. Fluorine Chem.*, 2015, **180**, 117.
15 V. P. Tolstoy and L. B. Gulina, *J. Nano-Electron. Phys.*, 2013, **5**, 01003.
16 V. P. Tolstoy and L. B. Gulina, *Langmuir*, 2014, **30**, 8366.
17 V. P. Tolstoi and L. B. Gulina, *Russ. J. Gen. Chem.*, 2013, **83**, 1635 (*Zh. Obshch. Khim.*, 2013, **83**, 1409).
18 S. M. Aldoshin and N. A. Sanina, *Russ. Chem. Rev.*, 2016, **85**, 1185.

19 O. G. Ellert, M. V. Tsodikov and V. M. Novotortsev, *Russ. Chem. Rev.*, 2010, **79**, 693 (*Usp. Khim.*, 2010, **79**, 758).
20 A. M. Abakumov, M. G. Rozova and E. V. Antipov, *Russ. Chem. Rev.*, 2004, **73**, 847 (*Usp. Khim.*, 2004, **73**, 917).
21 I. V. Baklanova, V. N. Krasil'nikov, O. I. Gyrdasova and L. Yu. Buldakova, *Mendeleev Commun.*, 2016, **26**, 335.
22 V. A. Drits, B. Lanson and A. C. Gaillot, *Am. Mineral.*, 2007, **92**, 771.
23 ICDD (International Centre for Diffraction Data), http://www.icdd.com. PDF (Powder Diffraction File) # 00-018-0802.
24 J. W. Murray, *J. Colloid Interface Sci.*, 1974, **46**, 357.
25 H. Hu and R. G. Larson, *J. Phys. Chem. B*, 2006, **110**, 7090.
26 I. F. Efremov, *Periodicheskie kolloidnye struktury* (*Periodic Colloidal Structures*), Khimiya, Leningrad, 1971 (in Russian).
27 H. Brune, C. Romainczyk, H. Röder and K. Kern, *Nature*, 1994, **369**, 469.
28 V. Fleury, *Nature*, 1997, **390**, 145.

Received: 6th May 2019; Com. 19/5913